the plant journal

SEB Society for Experimental Biology

The Plant Journal (2016) **88,** 120–131 doi: 10.1111/tpj.13265

EXA1, a GYF domain protein, is responsible for loss-of-susceptibility to plantago asiatica mosaic virus in *Arabidopsis thaliana*

Masayoshi Hashimoto, Yutaro Neriya, Takuya Keima, Nozomu Iwabuchi, Hiroaki Koinuma, Yuka Hagiwara-Komoda[†], Kazuya Ishikawa[§], Misako Himeno, Kensaku Maejima, Yasuyuki Yamaji and Shigetou Namba*

Laboratory of Plant Pathology, Department of Agricultural and Environmental Biology, Graduate School of Agricultural and Life Sciences, University of Tokyo, 1-1-1 Yayoi, Bunkyo-ku, Tokyo 113-8657, Japan

Received 7 April 2016; revised 24 June 2016; accepted 6 July 2016; published online 19 September 2016.
*For correspondence (e-mail anamba@mail.ecc.u-tokyo.ac.jp).
[†]Present address: Department of Sustainable Agriculture, Rakuno Gakuen University, Ebetsu, Hokkaido 069-8501, Japan.
[§]Present address: Department of Botany, Graduate School of Science, Kyoto University, Kyoto 606-8502, Japan.

SUMMARY

One of the plant host resistance machineries to viruses is attributed to recessive alleles of genes encoding critical host factors for virus infection. This type of resistance, also referred to as recessive resistance, is useful for revealing plant–virus interactions and for breeding antivirus resistance in crop plants. Therefore, it is important to identify a novel host factor responsible for robust recessive resistance to plant viruses. Here, we identified a mutant from an ethylmethane sulfonate (EMS)-mutagenized Arabidopsis population which confers resistance to plantago asiatica mosaic virus (PlAMV, genus *Potexvirus*). Based on map-based cloning and single nucleotide polymorphism analysis, we identified a premature termination codon in a functionally unknown gene containing a GYF domain, which binds to proline-rich sequences in eukaryotes. Complementation analyses and robust resistance to PlAMV in a T-DNA mutant demonstrated that this gene, named *Essential for poteXvirus Accumulation 1* (*EXA1*), is indispensable for PlAMV infection. *EXA1* contains a GYF domain and a conserved motif for interaction with eukaryotic translation initiation factor 4E (eIF4E), and is highly conserved among monocot and dicot species. Analysis using qRT-PCR and immunoblotting revealed that *EXA1* was expressed in all tissues, and was not transcriptionally responsive to PlAMV infection in Arabidopsis plants. Moreover, accumulation of PlAMV and a PlAMV-derived replicon was drastically diminished in the initially infected cells by the *EXA1* deficiency. Accumulation of two other potexviruses also decreased in *exa1-1* mutant plants. Our results provided a functional annotation to GYF domain-containing proteins by revealing the function of the highly conserved *EXA1* gene in plant–virus interactions.

Keywords: recessive resistance, EXA1, plantago asiatica mosaic virus, *Potexvirus*, GYF domain, *Arabidopsis thaliana*, plant–virus interactions.

INTRODUCTION

Plant host resistance to viruses can be classified into two categories: resistance mediated by dominant disease resistance (R) genes; and resistance attributed to recessive alleles of genes encoding host factors that are critical for viral infection. The latter, which is equivalent to the loss-of-susceptibility in mutagenized plants, has been conventionally referred to as recessive resistance. Recessive resistance is widely exploited in many crops because of its durability (Robaglia and Caranta, 2006; Truniger and Aranda, 2009; Wang and Krishnaswamy, 2012). In fact, approximately half of the virus resistance alleles of crops are recessive (Kang *et al.*, 2005). Therefore, research on a host factor responsible for loss-of-susceptibility would be beneficial both for understanding plant–virus interactions and for breeding for antiviral resistance.

Since plant viruses have a limited coding capacity, they employ many host factors to establish their infection. Previous studies have identified host factors and revealed their functions in the virus life cycle (Hyodo and Okuno, 2014; Heinlein, 2015; Sanfaçon, 2015). Disruptions of some of these host factors impair virus infection without any harmful effects on plants (Nishikiori *et al.*, 2011; Mine

et al., 2012). A few studies have succeeded in isolating loss-of-susceptibility mutants to plant viruses using *Arabidopsis thaliana* mutant screens. Through such forward genetic approaches, host factors that are critical for the virus infection process have been isolated from the model plant Arabidopsis*:* translation initiation factor eIF4E (Yoshii *et al.*, 2004), eIF(iso)4E (Lellis *et al.*, 2002), and the TOM1, TOM2A, and TOM3 proteins (Yamanaka *et al.*, 2000, 2002*;* Tsujimoto *et al.*, 2003). Other host factors critical for virus infection have been isolated from ecotypes with natural recessive resistance: *PDIL5-1* from barley and *cPGK* from the *A. thaliana* Cvi-0 ecotype (Ouibrahim *et al.*, 2014; Yang *et al.*, 2014).

The most extensively studied host factors responsible for recessive resistance are the translation initiation factors eIF4E and eIF4G, and their isoforms. Lellis *et al.* (2002) first reported eIF(iso)4E as a factor responsible for loss-of-susceptibility to a potyvirus based on an Arabidopsis mutant screen. Subsequently, a number of studies demonstrated that recessive alleles in several crop species correspond to mutations in eIF4E/4G and their isoforms using candidate gene approaches (Ruffel *et al.*, 2002, 2005; Nicaise *et al.*, 2003). It is well known that eIF4E/4G provides robust resistance, mainly against potyviruses and several other viruses (Albar *et al.*, 2006; Nieto *et al.*, 2006). Moreover, many research efforts on their roles in viral infection provided valuable insights into sophisticated viral infection strategies (Yoshii *et al.*, 2004*;* Wang and Krishnaswamy, 2012*;* Sanfaçon, 2015). The development of research on the role of eIF4E/4G in viral infection suggests the importance of identifying a critical host factor that is widely conserved in plants through an Arabidopsis mutant screen for a robust resistance mutant.

The potexviruses constitute a group of single-stranded, positive-sense RNA viruses containing potato virus X (PVX) as the type species. Some of the potexviruses, such as pepino mosaic virus and cymbidium mosaic virus, cause severe crop production losses (Hanssen and Thomma, 2010; Koh *et al.*, 2014). Therefore, it is necessary to identify and characterize fundamental host factors involved in potexvirus infection for future development of a new technology to manage potexviruses. Several host factors have been identified from tobacco plants using bamboo mosaic virus (BaMV) as a model virus (Lin *et al.*, 2007; Huang *et al.*, 2012; Liou *et al.*, 2015). However, an Arabidopsis mutant screen to isolate a novel host factor responsible for susceptibility to potexvirus infection has not been conducted to date.

As a step toward this goal, we recently showed that plantago asiatica mosaic virus (PlAMV), a potexvirus, infects *A. thaliana* efficiently. We developed green fluorescence protein-tagged PlAMV (PlAMV–GFP), which enables us to perform a high-throughput screen for a resistance locus to potexviruses using *A. thaliana* (Yamaji *et al.*, 2012; Minato *et al.*, 2014). In this study, we aimed to identify a host factor by screening for an Arabidopsis mutant resistant to PlAMV–GFP. We identified EXA1 as a host factor that is critical for infection by several potexviruses. EXA1 contains a GYF domain, which acts as an adaptor that binds to proline-rich sequences (PRSs) in eukaryotic cells (Kofler and Freund, 2006). The molecular function of GYF domain proteins in plants is largely unknown, especially whether they are involved in cellular responses to pathogen attack. Our results demonstrated that *EXA1* is widely conserved among monocot and dicot species, and that EXA1-mediated resistance significantly impairs virus accumulation at the single cell level. Based on our results, we discuss the potential relevance of EXA1-mediated resistance to other plant species and other viruses, and the molecular role of EXA1 in plant–virus interactions.

RESULTS

Isolation of an Arabidopsis mutant resistant to PlAMV

To identify a mutant with loss-of-susceptibility to PlAMV, we screened approximately 10 000 plants of the *A. thaliana* ecotype Columbia (Col-0) which were subjected to ethyl methanesulfonate (EMS) mutagenesis. PlAMV–GFP was inoculated onto plants and viral infection was monitored by the proliferation of the GFP fluorescence of PlAMV–GFP. In susceptible Col-0 plants, the GFP fluorescence of PlAMV–GFP was clearly observed in the inoculated leaves and the upper leaves at 4 and 16 days post-inoculation (dpi), respectively. After a two-round inoculation test, we isolated a mutant (line E10773) that conferred resistance to PlAMV–GFP. In addition to the virus resistance phenotype, the E10773 mutant exhibited other developmental phenotypes, such as round-shaped expanded leaves, weak sterility, and delayed vegetative growth (Figure S1(a)). However, the progeny of the E10773 mutant backcrossed twice to Col-0 (ECC mutant), which retained the resistance phenotype (Figure 1(a)), did not exhibit such developmental phenotypes, except for mild dwarfism (Figure S1(a)). These results indicated that the resistance phenotype of the isolated mutant was genetically unrelated to other developmental abnormalities (Figure S1(a)).

To analyze the resistance phenotype of the E10773 mutant in detail, we mechanically inoculated PlAMV–GFP onto the ECC mutant. At 4 dpi, GFP fluorescence of PlAMV–GFP was clearly observed in the inoculated Col-0 leaves, but no GFP fluorescence was observed in the ECC mutant (Figure 1(b)). This result was confirmed by RT-PCR detection of PlAMV–GFP accumulation in the inoculated leaves. Consistent with these results, PlAMV–GFP infection was not observed in the upper leaves of the ECC mutant plants (Figure 1(a, c)). These results demonstrated that the ECC mutant did not support PlAMV–GFP accumulation in

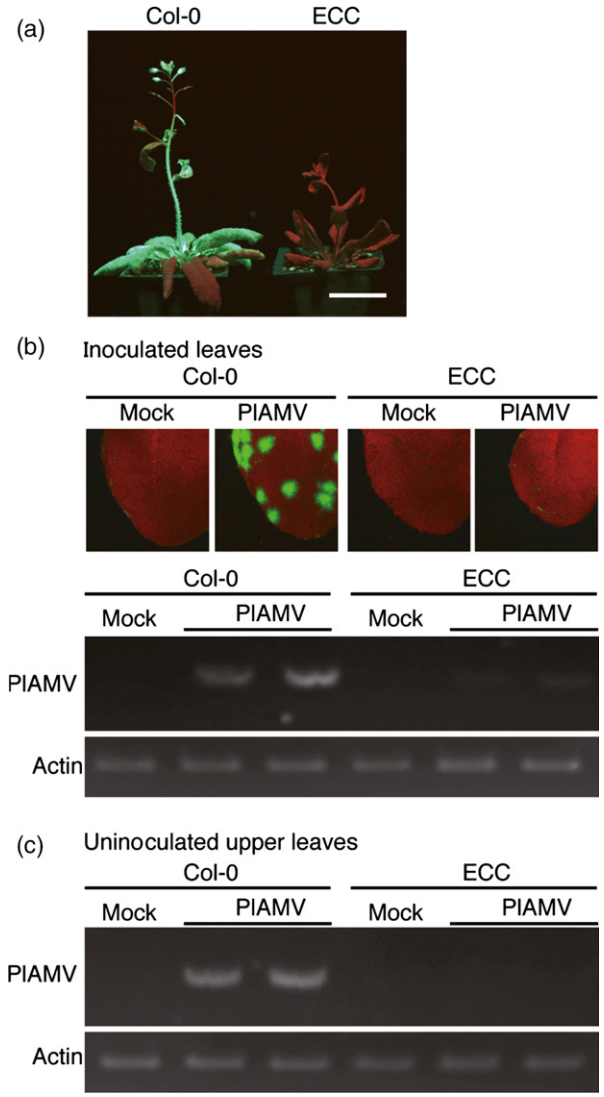

Figure 1. Resistance phenotype against PlAMV–GFP in ECC mutant plants.
(a) GFP fluorescence of PlAMV–GFP in the whole plants of Col-0 and ECC mutant. PlAMV–GFP was mechanically inoculated onto both genotypes. Photographs were taken at 19 days post-inoculation (dpi) under UV light. Bar = 2 cm.
(b) (upper panels) GFP fluorescence of PlAMV–GFP in the inoculated leaves of the ECC mutant and Col-0. PlAMV–GFP was inoculated mechanically onto ECC and Col-0 plants. Photographs were taken at 4 days post-inoculation (dpi) using the GFP pass filter of a fluorescence microscope. (lower two panels) Detection of PlAMV–GFP accumulation in the inoculated leaves by RT-PCR. Total RNA was extracted at 4 dpi.
(c) PlAMV–GFP detection by RT-PCR was performed for the uninoculated upper leaves at 14 dpi.

the inoculated leaves, resulting in complete resistance to systemic PlAMV infection.

To examine the genetic features of the E10773 resistant phenotype, we analyzed the segregation ratio of resistance phenotypes to PlAMV–GFP, using the F1 and F2 progeny of the ECCC mutant, which was backcrossed three times to Col-0. All of the F1 progeny were susceptible to PlAMV–GFP (Table 1). Among 83 plants of the F2 progeny, 16 plants (19.3%) were resistant and 67 (80.7%) plants were susceptible. This ratio (16 resistant to 67 susceptible) was close to the expected 1:3 ratio (Table 1), suggesting that the resistance phenotype of E10773 was governed by a single recessive locus.

Table 1 Inoculation test of PlAMV–GFP in E10773 and related plants

Plants[a]	Resistant	Susceptible
E10773	15	0
Col-0	0	16
ECCC F1	0	38
ECCC F2	16[b]	67[b]
L*er*	0	13
E10773 × L*er* F1	0	9
E10773 × L*er* F2	111	854

[a]The listed plants were inoculated with PlAMV–GFP by agroinfiltration. Viral infection was evaluated by the presence (Susceptible) or absence (Resistant) of GFP fluorescence from PlAMV–GFP in systemic leaves at 14 dpi.
[b]Pearson's chi-squared test with Yates' continuity correction using R software version 3.1.2. χ^2 (3:1) = 0.5565; P = 0.4557.

Identification of a host gene whose expression is correlated with resistance to PlAMV

To identify the locus responsible for the resistance phenotype in the E10773 mutant, we performed map-based cloning based on simple sequence length polymorphism (SSLP) markers and single nucleotide polymorphism (SNP) markers. Since the resistance phenotype was genetically recessive, resistant F2 plants from a cross of E10773 and L*er* were selected for map-based cloning (Table 1). First, among 20 SSLP markers that distinguish Col-0 and L*er*, we found that the resistance locus was linked tightly to the SSLP marker CIW9 between nga76 and JV65/66 on chromosome 5. To further perform linkage analysis using SNP markers, we employed four SNP markers (Table S1) located between the SSLP markers, nga76 and JV65/66. As a result, we found that the resistance locus was located within a 4.7-Mb region between two SNP markers, SGCSNP204 and Ler143 (Figure 2(a)).

Given that mutagenesis by EMS treatment generally causes G-to-A or C-to-T transitions in the plant genome, we expected that these types of SNPs could disrupt some genes found in the resistant EC mutant, a single backcrossed line of the E10773 mutant to Col-0. To identify an SNP residue linked to the resistance phenotype within the 4.7-Mb region of the EC genome, we analyzed SNPs in the region using MiSeq, a next-generation sequencing platform. Genomic DNAs extracted from five seedlings of EC mutants were processed to construct DNA libraries and sequenced. The obtained sequences were aligned to the public data of the Col-0 TAIR9 reference genome, and they

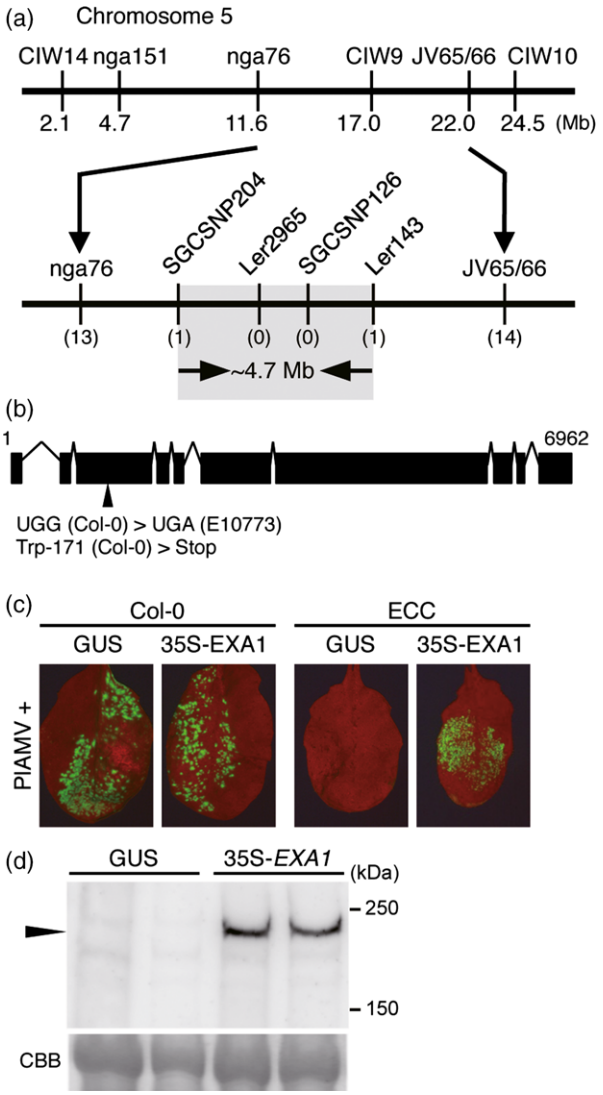

Figure 2. Identification of *EXA1.*

(a) Map-based method for delimiting the resistance locus. Horizontal line indicates a part of chromosome 5 and SSLP markers on chromosome 5, and the locations (Mb) are indicated at the top. Four SNP markers employed to further delimit the resistance locus are shown below. The numbers of resistant F2 plants at each marker locus are represented in parentheses.

(b) The intron and exon structure of the *EXA1* (AT5G42950) gene. Black boxes indicate exons. The locations of the identified SNP and the T-DNA in the resistance mutants are shown at the bottom. The *EXA1* mRNA (GenBank accession number: LC130495) consists of a 5145-nucleotide (nt) open reading frame, an 81-nt 5′-untranslated region (UTR), and a 272-nt 3′-UTR.

(c) Complementation of PlAMV–GFP infection by transient expression of *EXA1* driven by the 35S promoter in the ECC mutant. PlAMV–GFP and 35S-EXA1 (or pBI121 binary vector expressing GUS) were coinfiltrated into cells at an optical densities (600 nm) of 0.01 and 0.5, respectively. PlAMV–GFP accumulation was monitored using GFP fluorescence. Photographs were taken at 3 dpi.

(d) Confirmation of EXA1 expression by immunoblot analysis. 35S-*EXA1* was agroinfiltrated into *Nicotiana benthamiana* leaves. Total protein was extracted at 3 dpi. Arrowhead indicates EXA1-specific signals. A protein size marker is shown at the right side of the panel. Two replicates are shown for each treatment.

covered approximately 75.3% (3.54 Mb) of the 4.7-Mb region. Relative to the Col-0 genome, we detected 69 SNPs in the 4.7-Mb region of the EC genome which were common to all of the sequence data obtained from at least two seedlings of the EC mutant. We selected the SNPs located in the region in which some genes were encoded (exon or intron), which exhibited the canonical EMS-induced nucleotide changes. Further, eight SNPs that were located in exon regions but caused no amino acid substitutions were eliminated, leaving 30 SNPs that could affect the functions of 29 distinct genes (Table S2). Among the 29 candidate genes, the only apparent defect we found was a predicted premature termination codon caused by an SNP in the third exon region of the AT5G42950 gene, a GYF domain-containing gene (Figure 2(b)). Since our following results indicated that AT5G42950 was indispensable for PlAMV infection, we designated this gene as *Essential for poteXvirus Accumulation 1* (*EXA1*).

To confirm whether the premature termination codon stopped EXA1 translation as predicted, we raised an antibody against the amino terminus of the EXA1 protein and attempted to detect EXA1 protein expression in E10773, ECC mutant, and Col-0 plants by immunoblot analysis. A specific signal of ca. 190 kDa, which corresponds to the estimated molecular mass of EXA1 (187.6 kDa), was detected in Col-0, but not in the E10773 mutant or the ECC mutant (Figure S1(b)), suggesting that absence of EXA1 is consistent with the resistance phenotype.

To test whether EXA1 expression complemented PlAMV accumulation in the E10773 mutant, we performed a complementation assay using transient gene expression. 35S-*EXA1* was introduced using an *Agrobacterium*-mediated transient expression system into the ECC mutant and Col-0 along with PlAMV–GFP. As a control, we confirmed that transient EXA1 expression did not affect the propagation of the GFP fluorescence of PlAMV–GFP in Col-0 plants at 3 dpi (Figure 2(c, d)). In the ECC mutant plants, although no GFP fluorescence of PlAMV–GFP was observed in the mock-inoculated leaves, accumulation of PlAMV–GFP was clearly observed in the EXA1-expressing leaves (Figure 2(c)). These results suggested that transient expression of full-length EXA1 supported PlAMV–GFP infection in the ECC mutant.

An *EXA1* T-DNA mutant, *exa1-1,* confers resistance to PlAMV

To investigate whether loss-of-function of *EXA1* is responsible for resistance to PlAMV, we obtained a T-DNA insertion mutant of *EXA1* (SALK_005994C, hereafter *exa1-1;* Figure S1(a)). EXA1 protein expression was not detected in *exa1-1,* similar to the E10773 and ECC mutants (Figures 3(a) and S1(b)). When PlAMV–GFP was inoculated

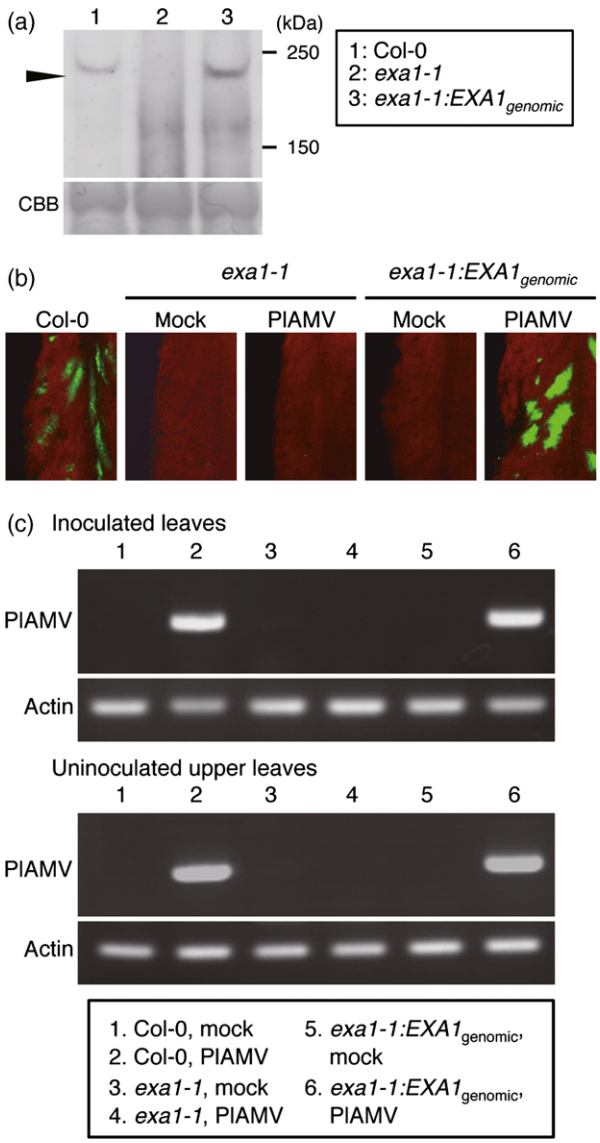

Figure 3. Resistance phenotype of *exa1-1* T-DNA insertion mutant.
(a) Immunoblot analysis to detect expression of EXA1 in *exa1-1* and *exa1-1:EXA1*$_{genomic}$ transformed lines. Arrowhead indicates EXA1-specific signals. Protein size marker is shown at the right side of the panel.
(b) Resistance phenotype of *exa1-1* mutant against PIAMV–GFP and restoration of PIAMV–GFP infection in *exa1-1:EXA1*$_{genomic}$. Photographs of GFP fluorescence in the inoculated leaves were taken at 4 dpi.
(c) Detection of PIAMV–GFP accumulation by RT-PCR in the inoculated (upper two panels) and upper leaves (lower two panels) of *exa1-1* and *exa1-1:EXA1*$_{genomic}$. Total RNA was extracted from the leaves inoculated mechanically with PIAMV–GFP and from the upper leaves at 4 and 14 dpi, respectively.

mechanically onto the *exa1-1* mutant, GFP fluorescence of PIAMV–GFP was not observed in the inoculated leaves (Figure 3(b)). The decrease of PIAMV accumulation in the inoculated leaves of *exa1-1* was confirmed by RT-PCR (Figure 3(c)). PIAMV–GFP did not accumulate in the upper leaves of the *exa1-1* mutant, indicating that systemic PIAMV–GFP infection was abolished by the lack of *EXA1* (Figure 3(c)). Next, we constructed complemented lines transformed with the genomic fragment of *EXA1* (*exa1-1:EXA1*$_{genomic}$). Comparable EXA1 expression was confirmed in *exa1-1:EXA1*$_{genomic}$ complemented lines (Figure 3(a)). PIAMV infection was observed in both the inoculated and upper leaves of *exa1-1:EXA1*$_{genomic}$ similar to that in Col-0 (Figure 3(b, c)). These results demonstrated that EXA1 was indispensable for PIAMV infection in *A. thaliana.* Furthermore, absence of EXA1 expression was correlated with the resistance phenotype in mutants derived from E10773 and the T-DNA insertion mutant *exa1-1,* suggesting that the E10773 resistance to PIAMV was due to the lack of EXA1.

Characterization of the *exa1-1* mutant

R-mediated resistance, one of the major resistance mechanisms of plants against viruses, is associated with several defense responses, such as cell death caused by the hypersensitive response (HR) (Moffett, 2009). The GYF domain is known to function in cellular signaling pathways in animal cells (Nishizawa *et al.*, 1998; Giovannone *et al.*, 2003). If EXA1 negatively regulates the signaling pathway of R-mediated resistance, the *exa1-1* mutant would exhibit an elevated defense phenotype, such as the phenotype of *accelerated cell death 6* (*acd6*) (Rate *et al.*, 1999). We measured hydrogen peroxide production and cell death using 3,3′-diaminobenzidine (DAB) staining and trypan blue staining, respectively. In both experiments, no signal was observed in *exa1-1* mutants as well as in Col-0 (Figure S2 (a, b)). Expression of defense-related genes in *exa1-1* mutant was evaluated by quantitative RT-PCR (qRT-PCR). *PR-1, PR-2* and *PR-5* are known to be upregulated during defense responses (Uknes *et al.*, 1992). In *exa1-1* mutant, expression levels of *PR-1* and *PR-2* were not upregulated compared with Col-0, whereas *PR-5* was increased slightly (Figure S2(c)). The expression patterns of *PR-1* and *PR-5* in *exa1-1* mutant are apparently different from those during R-mediated resistance (Takahashi *et al.*, 2004). These results indicated that the *exa1-1* mutant does not exhibit an elevated defense phenotype similar to that in R-mediated resistance.

EXA1 is a GYF domain-containing genes belonging to the SMY2 subgroup in *A. thaliana*

A single GYF domain was predicted as a functional domain in the EXA1 amino acid sequence (Figure 4(a)). The GYF domain, composed of approximately 50 amino acids, functions as an adapter which binds to PRSs (Kofler and Freund, 2006). The GYF domain is widely conserved in eukaryotes including plants, yeast, mice, and humans. In the EMBL database, we found nine genes in the Arabidopsis genome which possess putative GYF domains. *EXA1* was most similar to two genes, *AT1G24300* and *AT1G27430* (63.5 and 67.3% identities in the GYF domain;

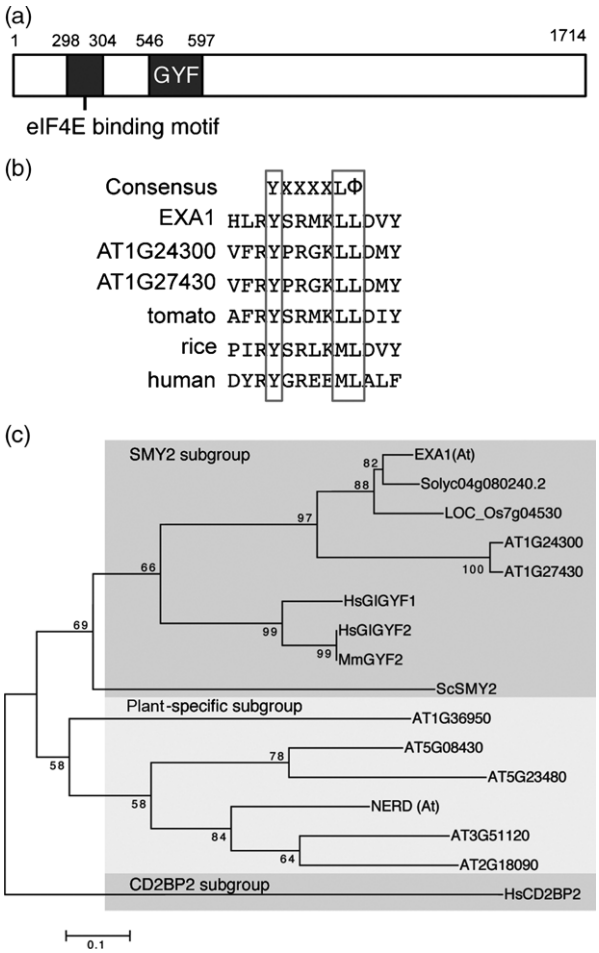

Figure 4. Domain structure and phylogenetic analysis of *EXA1.*
(a) Predicted functional domain structure of *EXA1.* White and grey boxes indicate the *EXA1* coding region and domains, respectively. Numbers on the top indicate the amino acid positions of the domains in *EXA1.*
(b) Sequence alignment of the deduced eIF4E-binding motif found in *EXA1* and its homologs and orthologs. Tomato, Solyc04g080240.2; rice, LOC_Os7g04530; and human, HsGIGYF2. X and Φ indicates any and hydrophobic amino acid, respectively.
(c) Phylogenetic analysis of amino acid sequences of GYF domains. Phylogenetic tree generated using the neighbour-joining method with pair wise deletion and 1000 replicates. HsCD2BP2 is included as an outgroup.

19.9 and 20.0% identities in the full-length amino acid sequences, respectively). Next, we performed a BLAST search using the GYF domain sequence of EXA1 as a query, and found that genes closely related to *EXA1* were also encoded in tomato and rice. Sequence identities of the *EXA1* gene with these genes (90.2 and 64.3% in the GYF domain; 48.1 and 36.0% in the full-length amino acid sequences, respectively) exhibited significantly high values and higher than those of Arabidopsis *EXA1*-like genes (*AT1G24300* and *AT1G27430*), suggesting that the tomato and rice genes were orthologs of *EXA1.* The GYF domain sequence of EXA1 also showed high identity to human *HsGIGYF2* (53.1%), which is involved in translational regulation (Morita *et al.*, 2012). Although no sequence similarity was detected, excluding the GYF domain, compared with *HsGIGYF2,* a region similar to the eIF4E-binding motif, Y-X_4-L-L, was found in the N-terminal region of EXA1 (Figure 4(a, b)). This protein–protein interaction motif was also found in *HsGIGYF2* (Morita *et al.*, 2012), the tomato and rice *EXA1* orthologs and in two Arabidopsis EXA1-like genes, suggesting that *EXA1* and its related plant genes might share similar functions with mammalian GIGYF2.

We performed a phylogenetic analysis of the GYF domain amino acid sequences of EXA1 and other GYF domain-containing proteins (Figure 4(c)). As described earlier (Freund *et al.*, 2002), GYF domains are grouped into three subgroups: the SMY2, plant-specific, and CD2BP2 subgroups. Nine Arabidopsis proteins possessing the GYF domain were divided into plant-specific or SMY2 subgroups. NERD, the only functionally annotated Arabidopsis GYF domain protein (Pontier *et al.*, 2012), is classified into the plant-specific subgroup. In contrast, *EXA1* belonged to the SMY2 subgroup similar to *HsGIGYF2,* together with tomato and rice orthologs and two other Arabidopsis *EXA1*-like genes. Consistent with sequence identities, phylogenetic analysis showed that *EXA1* was more closely related to the tomato and rice orthologs than the two Arabidopsis *EXA1*-like genes. These results suggested that *EXA1* might have been generated from a deduced SMY2-type ancestor gene before dicots and monocots diverged.

EXA1 expression pattern

To obtain insights into the function of EXA1 in plants, we investigated the expression levels of *EXA1* transcripts and translation products in specific plant tissues. Total RNAs or proteins collected from 30-day-old plants were used in qRT-PCR or immunoblot analysis. In the immunoblot analysis, the *exa1-1* mutant was used as a negative control. qRT-PCR and immunoblot analysis showed that *EXA1* mRNA and protein were expressed in all plant tissues (Figure 5(a, b)). In particular, *EXA1* transcript levels were higher in flowers and lower in roots, leaves, and stems (Figure 5(a)). In contrast, levels of *EXA1* translation products tended to be higher in leaves or flowers and lower in roots and stems (Figure 5(b)). These results suggested that *EXA1* mRNA and protein were consistently expressed in all of the tissues.

To obtain more insights into the role of EXA1 in plants, we also tested expression levels of *EXA1* transcripts in the leaves inoculated with PlAMV–GFP. Generally, when viruses invade plants during susceptible interactions, transcriptional levels of diverse plant genes change dramatically (Postnikova and Nemchinov, 2012). After PlAMV–GFP was inoculated onto Col-0, total RNAs were extracted at several time points from the inoculated leaves and *EXA1* transcript accumulation levels were measured by qRT-PCR. The expression level of *EXA1* transcripts was consistent compared with that of mock-inoculated leaves at all time

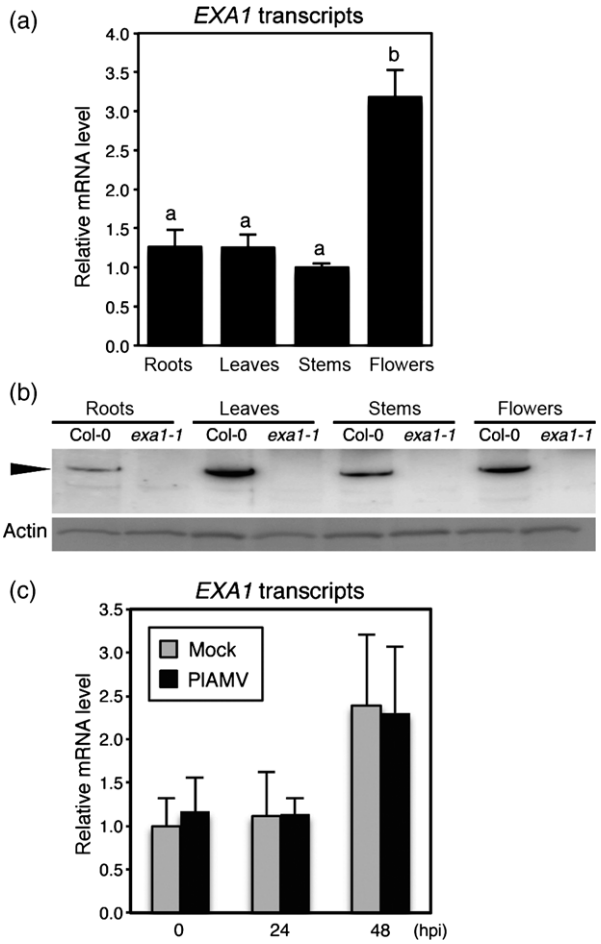

Figure 5. Expression analysis of *EXA1* transcripts and translation products.
(a) Tissue-specific expression levels of *EXA1* transcripts in Col-0. *EXA1* transcript levels were measured by qRT-PCR using total RNA extracted from the indicated tissues. Bars and error bars indicate mean values and standard deviations of three replicates relative to the value in leaves. Different letters at the top of the bars indicate significant differences (Student's *t*-test, $P < 0.05$).
(b) Tissue-specific levels of EXA1 proteins. Total protein was extracted from Col-0 and *exa1-1* tissues, and immunoblot analysis was performed using anti-EXA1 antiserum (upper panel). Actin protein levels determined using anti-Actin antibody are shown as loading controls at the bottom. Arrowhead indicates EXA1-specific signals.
(c) Expression profile of *EXA1* transcripts in virus-inoculated leaves. Total RNA was extracted from virus-inoculated leaves at the indicated time points. *EXA1* transcript levels were measured by qRT-PCR. Each bar indicates the mean value of the *EXA1* mRNA level from four replicates normalized to the Actin mRNA level. The mean value in mock-inoculated leaves at 0 h post-inoculation (hpi) was used as the standard.

points (Figure 5(c)). These results indicated that the level of *EXA1* transcription was not responsive to PlAMV infection.

PlAMV infection is impaired by EXA1-mediated resistance in the initially infected cells

Next, we aimed to determine which viral infection step was inhibited by EXA1-mediated resistance. In the initially infected cells, plant viruses translate replicases from their genomic RNAs, and the replicases and many host factors coordinately produce progeny genomic RNA molecules (Hyodo and Okuno, 2014), and subsequently genomic RNAs are transported to adjacent cells through plasmodesmata. When PlAMV–GFP was inoculated mechanically onto Col-0 plants, infection foci initially appeared at 3 dpi, and the size of the foci expanded in a time-dependent manner (Figure S3). In contrast, as also shown in Figure 3(b), no infection foci were observed in the *exa1-1* mutant at any time point (Figure S3), indicating that an infection step prior to cell-to-cell movement was abolished in the *exa1-1* mutant.

To determine whether PlAMV infection was influenced in the initially infected cells, we evaluated PlAMV accumulation in single cells of *exa1-1* and Col-0. Mesophyll protoplasts were isolated from the *exa1-1* mutant or Col-0 plants, and were transfected with a plasmid expressing PlAMV or 35S promoter-driven GFP (35S-GFP) along with 35S-Rluc as an internal control. Under our experimental condition, GFP fluorescence of 35S-GFP appeared in both Col-0 and *exa1-1* protoplasts at 1 dpi, indicating that there was no significant difference in the transfection efficiency between Col-0 and *exa1-1* protoplasts. Total RNAs were extracted at 3 dpi, and accumulation of PlAMV was compared between *exa1-1* mutant or Col-0 using qRT-PCR. PlAMV accumulation was significantly decreased in *exa1-1* protoplasts compared with Col-0 protoplasts (Figure 6(a)). Given that the viral genome synthesis in the initially infected cells solely depends on a viral replicase, RNA-dependent RNA polymerase (RdRp), among viral-encoded proteins, our results implied that the function of PlAMV RdRp is affected by the deficiency of EXA1. To test this possibility, we analyzed the accumulation of the 53U-RdRp, which is a PlAMV-derived replicon containing only RdRp gene and 5′ and 3′ untranslated regions required for genome replication (Komatsu *et al.*, 2011). When 53U-RdRp was transfected into ECC and *exa1-1,* the RNA accumulation level was significantly decreased in both ECC and *exa1-1* compared with Col-0 (Figure 6(b)). These results suggested that EXA1-mediated resistance impaired PlAMV infection through affecting the RdRp function in the initially infected cells.

The *exa1-1* mutant exhibits resistance to other potexviruses

To test the range of EXA1-mediated resistance, we examined whether other potexviruses could accumulate in *exa1-1* mutant plants as well as in Col-0. Alternanthera mosaic virus (AltMV), a potexvirus, infects Col-0 plants (Lim *et al.*, 2010; Iwabuchi *et al.*, 2016). AltMV was inoculated mechanically onto *exa1-1* and Col-0 plants, total RNAs were extracted from the inoculated leaves, and AltMV accumulation was monitored using qRT-PCR. At 4 dpi,

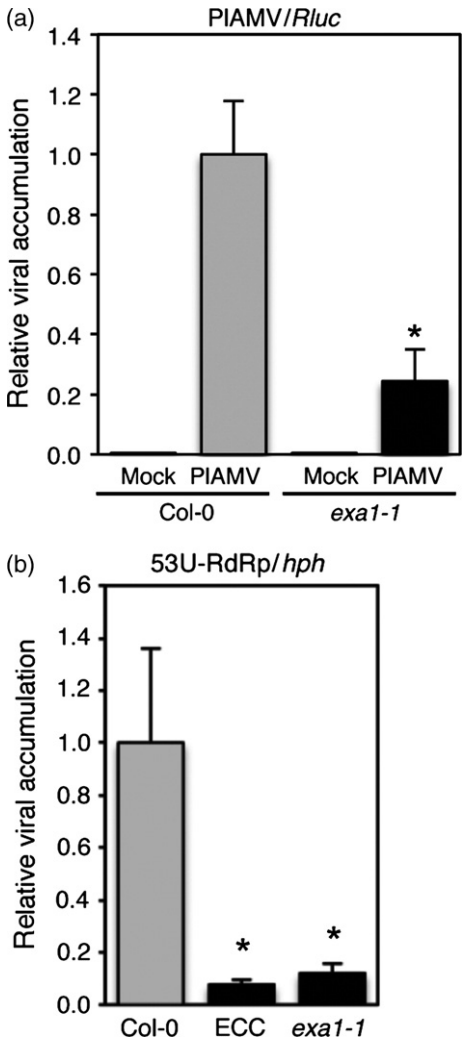

Figure 6. Influence of the deficiency of EXA1 on the cellular level accumulation of PlAMV.
(a) Quantification of PlAMV–GFP accumulation by qRT-PCR. Total RNA was extracted from protoplasts at 3 days after transfection. RLUC values were used as an internal control. Bars and error bars indicate mean values and standard errors of four replicates relative to the value in Col-0.
(b) Accumulation of 53U-RdRp replicon RNA in ECC and *exa1-1*. RNA level was quantified by qRT-PCR. Total RNA was extracted from leaves at 3 days after transfection with 53U-RdRp by particle bombardment. The values of *hph* gene encoded in the transfected plasmid were used as an internal control. Bars and error bars indicate mean values and standard errors of eight replicates relative to the value in Col-0. Asterisks indicate significant differences compared with Col-0 (Student's *t*-test, $P < 0.05$).

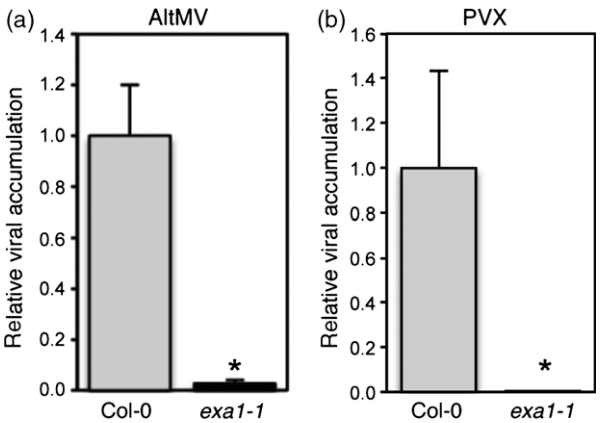

Figure 7. Inoculation of other potexviruses in the *exa1-1* mutant.
In (a) and (b), levels of AltMV and PVX accumulation, respectively, were evaluated using qRT-PCR. Bars and error bars indicate mean values and standard deviations of four replicates relative to the value in Col-0. Asterisks indicate significant differences compared with Col-0 (Student's *t*-test, $P < 0.05$).
(a) Sap prepared from AltMV-inoculated *N. benthamiana* was inoculated mechanically onto the *exa1-1* mutant. Total RNA was extracted from the inoculated leaves at 4 dpi.
(b) Purified virions of PVX BH strain were inoculated mechanically into the *exa1-1* mutant. Total RNA was extracted from the inoculated leaves at 7 dpi.

accumulation of AltMV significantly diminished in *exa1-1,* compared with Col-0 (Figure 7(a)). Another potexvirus, PVX, could not infect Col-0 plants systemically, but replicates in the initially infected cells of Col-0 plants (Jaubert *et al.*, 2011; Brosseau and Moffett, 2015). To compare the accumulation levels of PVX between *exa1-1* and Col-0, we performed qRT-PCR using total RNAs extracted from leaves inoculated with PVX (BH strain; Komatsu *et al.*, 2005). As shown in Figure 7(b), PVX accumulation was significantly diminished in *exa1-1* compared with Col-0. These results indicated that EXA1-mediated resistance is effective against at least these three potexviruses, including PlAMV. We further examined whether EXA1-mediated resistance impairs infection by other viruses unrelated to potexviruses. Turnip crinkle virus (TCV, *Carmovirus*), turnip yellow mosaic virus (TYMV, *Tymovirus*), and youcai mosaic virus (YoMV, *Tobamovirus*) were inoculated mechanically onto *exa1-1* and Col-0 plants. Symptoms specific for each virus appeared in *exa1-1* mutants, and all of the viruses were detected in the upper leaves of the *exa1-1* mutant using RT-PCR, as seen in Col-0 (Table S3). Together, these results indicated that the *exa1-1* mutant prevented accumulation of potexviruses, but did not affect systemic infection of other viruses.

DISCUSSION

In this study, we screened for a loss-of-susceptibility Arabidopsis mutant which is resistant to PlAMV, and showed that *EXA1* is indispensable for PlAMV infection. Several lines of evidence supported that disruption of *EXA1* is responsible for the loss-of-susceptibility phenotype of the E10773 mutant identified in this study. Moreover, EXA1-mediated resistance was also functional against the AltMV and PVX potexviruses and was robust enough to strictly impair PlAMV accumulation in the initially infected cells.

The GYF domain in *EXA1* is a conserved functional domain which binds PRSs in eukaryotes (Kofler and Freund, 2006). The GYF domain was originally identified in

the human CD2 binding protein 2 (CD2BP2) as the region responsible for binding to the T lymphocyte adhesion molecule CD2 (Nishizawa *et al.*, 1998). In animal or yeast cells, GYF domain-containing proteins are suggested to be involved in various cellular functions, including signal transduction pathways (Nishizawa *et al.*, 1998; Giovannone *et al.*, 2003), regulation of protein translation (Morita *et al.*, 2012), mRNA metabolism, and membrane trafficking (Ash *et al.*, 2010). In contrast, there have been no functional annotations for the GYF domain-containing proteins in plants, except for NERD, which is involved in the DNA methylation pathway (Pontier *et al.*, 2012). Our study suggests another functional aspect of a GYF domain protein in plant cells. Thus, it is necessary to further analyze the molecular function of EXA1 in the viral life cycle, as well as its intrinsic function in plant cells.

Our results revealed that the *EXA1* mRNA level was not affected in the early stage of PlAMV infection (Figure 5(c)). In addition, several defense responses associated with R-mediated resistance, one of the antiviral resistance mechanisms, were not activated constitutively in the *exa1-1* mutant plants (Figure S2), suggesting that EXA1-mediated resistance against PlAMV is independent of inducible defense responses. This hypothesis on EXA1-mediated resistance is substantiated by other results showing that systemic infection of other unrelated viruses was not compromised in the *exa1-1* mutant plants (Table S3). In the same way, preactivation or misregulation of other broad spectrum defense mechanisms, including RNA silencing, if any, is presumed to be unrelated to EXA1-mediated resistance against potexviruses. Taken together, these results suggest that EXA1 is a host factor essential for proliferation of potexviruses.

The translation initiation factors *eIF4E* and *eIF4G* and their isoforms, the most well studied recessive resistance gene in plants, are conserved in all eukaryotes, including higher plants (Joshi *et al.*, 2005; Sanfaçon, 2015). eIF4E-mediated resistance is effective against a wide range of potyviruses in various plant species (Wang and Krishnaswamy, 2012; Sanfaçon, 2015). *EXA1* is also highly conserved in both monocot and dicot species (Figure 4). EXA1-mediated resistance inhibited accumulation of three potexviruses (Figure 7). Therefore, disruption of the *EXA1* ortholog is expected to confer resistance to potexviruses in various plant species other than *A. thaliana.* In other words, it is possible that the role of EXA1 in viral infection is conserved across a wide range of plant–virus interactions.

In the Arabidopsis genome, there are two other *EXA1*-like genes (*AT1G24300* and *AT1G27430*), which belong to a clade distinct from *EXA1* (Figure 4). The phylogenetic relationship between EXA1 and EXA1-like genes resembles that between eIF4E and its isoform eIF(iso)4E (Joshi *et al.*, 2005). Given that eIF4E and eIF(iso)4E are used by different potyvirus species in a host plant (Truniger and Aranda, 2009; Sanfaçon, 2015), there might be functional differentiation among EXA1 and EXA1-like genes in the interactions with potexviruses.

Our results showed that PlAMV accumulation was significantly impaired in single cells by EXA1-mediated resistance (Figure 6(a)). Additionally, 53U-RdRp accumulation was significantly diminished by the deficiency of EXA1 (Figure 6(b)), indicating that EXA1-mediated resistance is effective against the viral accumulation solely depending on RdRp. EXA1-mediated resistance was conferred to AltMV and PVX, as well as to PlAMV. These results suggested that EXA1 is involved in an infection step(s) that relates to RdRp translation or its action, and is common to at least three potexviruses. Although the molecular function of EXA1 in the viral infection cycle remains unknown, we suggest two hypotheses based on previous findings.

One plausible explanation of EXA1 function is translational regulation. Previously, together with eIF4E/4G and their isoforms, EXA1 was identified in Arabidopsis plants as an interactor with m^7GTP-Sepharose, an analog of the cap structure of mRNA (Bush *et al.*, 2009). Human GIGYF2, which is closely related to EXA1, interacts with one of the eIF4E family members and is involved in translational regulation (Morita *et al.*, 2012). Consistent with this, we found an eIF4E-binding motif in the N-terminus of EXA1 (Figure 4). These results suggest that EXA1 is included in the translation initiation factor complex with eIF4E/4G or their isoforms to control mRNA translation via the interaction with eIF4E family proteins in plant cells. EXA1 might positively regulate the translation of another host factor that is required for potexvirus replication. Alternatively, since the potexvirus genomic RNAs have the same structure as host mRNA with a 5′ cap and a 3′ poly(A) tail, RdRp translation might be directly regulated by EXA1.

Another presumed function of EXA1 in potexvirus infection is based on the protein–protein interaction mediated by the GYF domain. Generally, the GYF domain is one of the functional domains which bind PRSs, and its protein–protein interaction is important for the function as an adaptor to express the roles of the partner proteins (Kofler and Freund, 2006). Thus, EXA1 might bind to the PRS of another host factor to assist the function of a viral factor. Previously, Kofler *et al.* (2005) isolated an Not4 homolog as an interactor of the GYF domain of EXA1. Not4, an E3 ubiquitin ligase with RNA-binding activities, is a component of the CCR4–NOT complex, which functions in deadenylation of eukaryotic mRNAs (Garneau *et al.*, 2007). In general, defective viral RNAs are frequently synthesized by error-prone replicases during the RNA virus replication step (Domingo and Holland, 1997). These findings lead to an interesting hypothesis that viruses generally recruit such mRNA surveillance machinery to promote their proliferation by effectively eliminating the defective RNAs or

utilizing the RNA-binding activity itself of Not4. Consistent with our hypothesis, brome mosaic virus (BMV) recruits the Lsm1-7–Pat1 complex, a component of the deadenylation-dependent mRNA decay machinery, for its genomic RNA translation and replication (Jungfleisch *et al.*, 2015). More recently, Meng and his colleagues demonstrated that the cytoplasmic exoribonuclease NbXRN4 also promotes BaMV accumulation in *Nicotiana benthamiana* (Lee *et al.*, 2016).

EXA1-mediated resistance completely impaired PlAMV accumulation in the initially infected cells (Figure 6). This result coincides with the robust resistance in both *exa1-1* and other allelic mutant plants in which PlAMV accumulation was not supported, even in the inoculated leaves. Several advantages of EXA1-mediated resistance mentioned above suggest that *EXA1* might be a potential candidate for molecular breeding for antiviral resistance in crops (Nieto *et al.*, 2007; Piron *et al.*, 2010). In future studies, it will be necessary to investigate whether EXA1-mediated resistance is actually applicable to other plant species including crops, or to other potexviruses and viruses in other genera closely related to potexviruses.

EXPERIMENTAL PROCEDURES

Plant materials

Growth conditions of *Arabidopsis thaliana* and *Nicotiana benthamiana* were described previously (Yamaji *et al.*, 2012). The Arabidopsis T-DNA mutant *exa1-1* (SALK_005994C) was provided by the Arabidopsis Biological Resource Center (ABRC; The Ohio State University, Columbus, Ohio, USA). To genotype *exa1-1,* T-DNA insertion was confirmed by two sets of PCRs, using Nd-EXA1-1330F and a T-DNA–specific primer, LBb1-3 (SALK Institute, San Diego, CA, USA), and NdEXA1-1330F and Xh-EXA1-2400R. Sequences of the primers used in this study are listed in Table S4. EMS mutagenesis of Arabidopsis Col-0 seeds was performed according to a general procedure described in Ishikawa *et al.* (1991).

RT-PCR and qRT-PCR

Primers used in RT-PCR and qRT-PCR are listed in Table S4. *Actin2* mRNA was used as an internal control for both RT-PCR and qRT-PCR (Okano *et al.*, 2014). In the protoplast and the particle bombardment experiments, *Renilla luciferase* (*RLUC*) and *hph* genes (a selectable marker contained in 53U-RdRp1 plasmid) were used as an internal control for qRT-PCR, respectively.

Genetic analysis

For map-based cloning of the resistance locus, genomic DNAs were isolated from resistant F2 plants produced from a cross of E10773 and L*er*. SSLP marker- and SNP-based mapping were conducted as described previously (Yamaji *et al.*, 2012). SNP markers and their primers are listed in Table S1.

SNP analysis using next-generation sequencing

SNP analysis using a next-generation sequencer (NGS), MiSeq (Illumina, San Diego, CA, USA), was conducted to identify an SNP site located within the genomic region between the SNP markers linked tightly to E10773 resistance according to the procedures by Uchida *et al.* (2011). Genomic DNA was extracted from EC mutant plants using the DNeasy Plant Mini kit (QIAGEN, Hilden, Germany), and used for sample preparation for sequencing following the manufacturer's procedures. Data processing for SNP analysis was performed using Illumina software and the Terminal application. The *A. thaliana* Col-0 genome (TAIR 9) was used as a reference. Alignment to TAIR 9 and SNP analysis was performed using MiSeq Reporter Software 1.3.17. The Integrative Genome Viewer was used to visualize the read alignment and confirm the SNP sites.

Plasmid constructs

A genomic fragment of *EXA1* was amplified by PCR using the primers, Kp-EXA1-upF and Nt-EXA1-down1kbR. PCR products were inserted into the Gateway Entry vector pENTA (Himeno *et al.*, 2010) between the *Kpn*I and *Not*I sites. The coding region of *EXA1* mRNA was amplified by RT-PCR using the Kp-EXA1-1F and Xh-EXA1-5145R primer pair. PCR products were inserted into pENTA between the *Kpn*I and *Xho*I sites. Each insert was subcloned into the pEarlyGate302 (Earley *et al.*, 2006) and pFAST02 vectors (Shimada *et al.*, 2010) to generate the $EXA1_{genomic}$ and 35S-*EXA1* constructs, respectively, using Gateway LR Clonase II Enzyme Mix (Thermo Fisher Scientific, Waltham, MA, USA). 35S-RLUC was constructed as below. The coding region of the *RLUC* gene was amplified by PCR using the 35S-GFP-rluc-1F and 35S-rluc-936R primers. The plasmid fragment was obtained from 35S-sGFP (Chiu *et al.*, 1996) using the 35S-GFP-down1F and 35S-GFP-up1R primers. The PCR-amplified *RLUC* was inserted downstream of the 35S promoter of the plasmid fragments using GeneArt Seamless Cloning and Assembly (Thermo Fisher Scientific).

Agroinfiltration and transformation of Arabidopsis

For agroinfilitration, binary plasmids were introduced into *Agrobacterium tumefaciens* EHA105. Transformation of Arabidopsis seedlings was performed according to the floral-dip method (Clough and Bent, 1998).

Antisera and immunoblotting

A partial cDNA fragment of *EXA1* was amplified by PCR from 35S-*EXA1* using the Nd-EXA1-1330F and Xh-EXA1-2022R primers. The PCR product was cloned into the pET30a vector between the *Nde*I and *Xho*I sites, and a recombinant His-tagged EXA1 fragment was expressed in *Escherichia coli* cells. The His-tagged recombinant protein, purified using a nickel affinity column, was injected into a rabbit to produce antiserum against EXA1. Immunoblotting was conducted as described previously (Hashimoto *et al.*, 2015). The Actin11 protein was detected using a mouse anti-Actin11 monoclonal antibody (Agrisera, Vännäs, Sweden).

DAB staining and trypan blue staining

These experiments were performed using the procedure described in our previous study (Komatsu *et al.*, 2010).

Preparation of protoplasts and plasmid transfection

Mesophyll protoplast preparation and plasmid transfection, using the polyethylene glycol-mediated method, were performed based on the procedure of Jin *et al.* (2001) with slight modification. A plasmid expressing PlAMV genome (Ozeki *et al.*, 2006) or 35S-GFP was transfected along with 35S-Rluc and pCAMBIA1301. The amount of plasmids used for each transfection is 10 μg.

Particle bombardment

Particle bombardment was performed using a Biolistic PDS 1000/He Particle Delivery System (Bio-Rad, Hercules, California, USA) according to the manufacturer's instruction. After p53U-RdRp1 (Komatsu *et al.*, 2011) was introduced into Arabidopsis leaves, leaves were incubated on an agarose plate at 23°C.

Accession numbers

LC130495 (*EXA1* mRNA, GenBank).

ACKNOWLEDGEMENTS

This research was supported by funds including JSPS KAKENHI Grant Number 25221201 (category 'S') to S.N. and Grant-in-Aid for JSPS Fellows (Grant Number 15J04093) to M. Hashimoto. All authors declare no conflict of interest.

SUPPORTING INFORMATION

Additional Supporting Information may be found in the online version of this article.

Figure S1. Morphological phenotypes of Arabidopsis mutants used in this study.

Figure S2. Analysis of several defense responses in *exa1-1* mutant.

Figure S3. Analysis of PlAMV–GFP cell-to-cell movement in *exa1-1.*

Table S1. SNP markers used in this study.

Table S2. Summary of SNP sites and the mutated genes identified in the 4.7-Mb region of chromosome 5.

Table S3. Inoculation tests of several plant viruses unrelated to potexviruses.

Table S4. Primers in this study.

REFERENCES

Albar, L., Bangratz-Reyser, M., Hébrard, E., Ndjiondjop, M.N., Jones, M. and Ghesquière, A. (2006) Mutations in the eIF(iso)4G translation initiation factor confer high resistance of rice to Rice yellow mottle virus. *Plant J.* **47**, 417–426.

Ash, M.R., Faelber, K., Kosslick, D., Albert, G.I., Roske, Y., Kofler, M., Schuemann, M., Krause, E. and Freund, C. (2010) Conserved beta-hairpin recognition by the GYF domains of Smy2 and GIGYF2 in mRNA surveillance and vesicular transport complexes. *Structure,* **18**, 944–954.

Brosseau, C. and Moffett, P. (2015) Functional and genetic analysis identify a role for Arabidopsis ARGONAUTE5 in antiviral RNA silencing. *Plant Cell*, **27**, 1742–1754.

Bush, M.S., Hutchins, A.P., Jones, A.M., Naldrett, M.J., Jarmolowski, A., Lloyd, C.W. and Doonan, J.H. (2009) Selective recruitment of proteins to 5′ cap complexes during the growth cycle in Arabidopsis. *Plant J.* **59**, 400–412.

Chiu, W., Niwa, Y., Zeng, W., Hirano, T., Kobayashi, H. and Sheen, J. (1996) Engineered GFP as a vital reporter in plants. *Curr. Biol.* **6**, 325–330.

Clough, S.J. and Bent, A.F. (1998) Floral dip: a simplified method for Agrobacterium-mediated transformation of Arabidopsis thaliana. *Plant J.* **16**, 735–743.

Domingo, E. and Holland, J.J. (1997) RNA virus mutations and fitness for survival. *Annu. Rev. Microbiol.* **51**, 151–178.

Earley, K.W., Haag, J.R., Pontes, O., Opper, K., Juehne, T., Song, K. and Pikaard, C.S. (2006) Gateway-compatible vectors for plant functional genomics and proteomics. *Plant J.* **45**, 616–629.

Freund, C., Kühne, R., Yang, H., Park, S., Reinherz, E.L. and Wagner, G. (2002) Dynamic interaction of CD2 with the GYF and the SH3 domain of compartmentalized effector molecules. *EMBO J.* **21**, 5985–5995.

Garneau, N.L., Wilusz, J. and Wilusz, C.J. (2007) The highways and byways of mRNA decay. *Nat. Rev. Mol. Cell Biol.* **8**, 113–126.

Giovannone, B., Lee, E., Laviola, L., Giorgino, F., Cleveland, K.A. and Smith, R.J. (2003) Two novel proteins that are linked to insulin-like growth factor (IGF-I) receptors by the Grb10 adapter and modulate IGF-I signaling. *J. Biol. Chem.* **278**, 31564–31573.

Hanssen, I.M. and Thomma, B.P. (2010) Pepino mosaic virus: a successful pathogen that rapidly evolved from emerging to endemic in tomato crops. *Mol Plant Pathol.* **11**, 179–189.

Hashimoto, M., Komatsu, K., Iwai, R. *et al.* (2015) Cell death triggered by a putative amphipathic helix of radish mosaic virus helicase protein is tightly correlated with host membrane modification. *Mol. Plant Microbe Interact.* **28**, 675–688.

Heinlein, M. (2015) Plant virus replication and movement. *Virology*, **479–480**, 657–671.

Himeno, M., Maejima, K., Komatsu, K., Ozeki, J., Hashimoto, M., Kagiwada, S., Yamaji, Y. and Namba, S. (2010) Significantly low level of small RNA accumulation derived from an encapsidated mycovirus with dsRNA genome. *Virology*, **396**, 69–75.

Huang, Y.W., Hu, C.C., Liou, M.R., Chang, B.Y., Tsai, C.H., Meng, M., Lin, N.S. and Hsu, Y.H. (2012) Hsp90 interacts specifically with viral RNA and differentially regulates replication initiation of Bamboo mosaic virus and associated satellite RNA. *PLoS Pathog.* **8**, e1002726.

Hyodo, K. and Okuno, T. (2014) Host factors used by positive-strand RNA plant viruses for genome replication. *J. Gen. Plant Pathol.* **80**, 123–135.

Ishikawa, M., Obata, F., Kumagai, T. and Ohno, T. (1991) Isolation of mutants of Arabidopsis thaliana in which accumulation of tobacco mosaic virus coat protein is reduced to low levels. *Mol. Gen. Genet.* **230**, 33–38.

Iwabuchi, N., Yoshida, T., Yusa, A., Nishida, S., Tanno, K., Keima, T., Nijo, T., Yamaji, Y. and Namba, S. (2016) Complete Genome Sequence of Alternanthera mosaic virus, isolated from Achyranthes bidentata in Asia. *Genome Announc.* **4**, pii: e00020-16. doi: 10.1128/genomeA.00020-16.

Jaubert, M., Bhattacharjee, S., Mello, A.F.S., Perry, K.L. and Moffett, P. (2011) ARGONAUTE2 mediates RNA-silencing antiviral defenses against Potato virus X in Arabidopsis1. *Plant Physiol.* **156**, 1556–1564.

Jin, J.B., Kim, Y.A., Kim, S.J., Lee, S.H., Kim, D.H., Cheong, G.W. and Hwang, I. (2001) A new dynamin-like protein, ADL6, is involved in trafficking from the trans-Golgi network to the central vacuole in Arabidopsis. *Plant Cell*, **13**, 1511–1526.

Joshi, B., Lee, K., Maeder, D.L. and Jagus, R. (2005) Phylogenetic analysis of eIF4E-family members. *BMC Evol. Biol.* **5**, 48.

Jungfleisch, J., Chowdhury, A., Alves-Rodrigues, I., Tharun, S. and Díez, J. (2015) The Lsm1-7-Pat1 complex promotes viral RNA translation and replication by differential mechanisms. *RNA*, **21**, 1469–1479.

Kang, B.C., Yeam, I. and Jahn, M.M. (2005) Genetics of plant virus resistance. *Annu. Rev. Phytopathol.* **43**, 581–621.

Kofler, M.M. and Freund, C. (2006) The GYF domain. *FEBS J.* **273**, 245–256.

Kofler, M.M., Motzny, K. and Freund, C. (2005) GYF domain proteomics reveals interaction sites in known and novel target proteins. *Mol. Cell Proteomics* **4**, 1797–1811.

Koh, K.W., Lu, H.C. and Chan, M.T. (2014) Virus resistance in orchids. *Plant Sci.*, **228**, 26–38.

Komatsu, K., Kagiwada, S., Takahashi, S. *et al.* (2005) Phylogenetic characteristics, genomic heterogeneity and symptomatic variation of five closely related Japanese strains of Potato virus X. *Virus Genes*, **31**, 99–105.

Komatsu, K., Hashimoto, M., Ozeki, J., Yamaji, Y., Maejima, K., Senshu, H., Himeno, M., Okano, Y., Kagiwada, S. and Namba, S. (2010) Viral-induced systemic necrosis in plants involves both programmed cell death and the inhibition of viral multiplication, which are regulated by independent pathways. *Mol. Plant Microbe Interact.* **23**, 283–293.

Komatsu, K., Hashimoto, M., Maejima, K. *et al.* (2011) A necrosis-inducing elicitor domain encoded by both symptomatic and asymptomatic Plantago asiatica mosaic virus isolates, whose expression is modulated by virus replication. *Mol. Plant Microbe Interact.* **24**, 408–420.

Lee, C.C., Lin, T.L., Lin, J.W., Han, Y.T., Huang, Y.T., Hsu, Y.H. and Meng, M. (2016) Promotion of Bamboo Mosaic virus accumulation in *Nicotiana benthamiana* by 5′→3′ exonuclease NbXRN4. *Front. Microbiol.* **6**, 1508. doi: 10.3389/fmicb.2015.01508.

Lellis, A.D., Kasschau, K.D., Whitham, S.A. and Carrington, J.C. (2002) Loss-of-susceptibility mutants of Arabidopsis thaliana reveal an essential role for eIF(iso)4E during potyvirus infection. *Curr. Biol.* **12**, 1046–1051.

Lim, H.S., Vaira, A.M., Domier, L.L., Lee, S.C., Kim, H.G. and Hammond, J. (2010) Efficiency of VIGS and gene expression in a novel bipartite potexvirus vector delivery system as a function of strength of TGB1 silencing suppression. *Virology*, **402**, 149–163.

Lin, J.W., Ding, M.P., Hsu, Y.H. and Tsai, C.H. (2007) Chloroplast phosphoglycerate kinase, a gluconeogenetic enzyme, is required for efficient accumulation of Bamboo mosaic virus. *Nucleic Acids Res.* **35**, 424–432.

Liou, M.R., Hu, C.C., Chou, Y.L., Chang, B.Y., Lin, N.S. and Hsu, Y.H. (2015) Viral elements and host cellular proteins in intercellular movement of Bamboo mosaic virus. *Curr. Opin. Virol.* **12**, 99–108.

Minato, N., Komatsu, K., Okano, Y., Maejima, K., Ozeki, J., Senshu, H., Takahashi, S., Yamaji, Y. and Namba, S. (2014) Efficient foreign gene expression in planta using a plantago asiatica mosaic virus-based vector achieved by the strong RNA-silencing suppressor activity of TGBp1. *Arch. Virol.* **159**, 885–896.

Mine, A., Hyodo, K., Tajima, Y., Kusumanegara, K., Taniguchi, T., Kaido, M., Mise, K., Taniguchi, H. and Okuno, T. (2012) Differential roles of Hsp70 and Hsp90 in the assembly of the replicase complex of a positive-strand RNA plant virus. *J. Virol.* **86**, 12091–12104.

Moffett, P. (2009) Mechanisms of recognition in dominant *R* gene mediated resistance. *Adv. Virus Res.* **75**, 1–33.

Morita, M., Ler, L.W., Fabian, M.R. *et al.* (2012) A novel 4EHP-GIGYF2 translational repressor complex is essential for mammalian development. *Mol. Cell. Biol.* **32**, 3585–3593.

Nicaise, V., German-Retana, S., Sanjuán, R., Dubrana, M.P., Mazier, M., Maisonneuve, B., Candresse, T., Caranta, C. and LeGall, O. (2003) The eukaryotic translation initiation factor 4E controls lettuce susceptibility to the Potyvirus Lettuce mosaic virus. *Plant Physiol.* **132**, 1272–1282.

Nieto, C., Morales, M., Orjeda, G. *et al.* (2006) An eIF4E allele confers resistance to an uncapped and non-polyadenylated RNA virus in melon. *Plant J.* **48**, 452–462.

Nieto, C., Piron, F., Dalmais, M. *et al.* (2007) EcoTILLING for the identification of allelic variants of melon eIF4E, a factor that controls virus susceptibility. *BMC Plant Biol.* **7**, 34.

Nishikiori, M., Mori, M., Dohi, K., Okamura, H., Katoh, E., Naito, S., Meshi, T. and Ishikawa, M. (2011) A host small GTP-binding protein ARL8 plays crucial roles in tobamovirus RNA replication. *PLoS Pathog.* **7**, e1002409.

Nishizawa, K., Freund, C., Li, J., Wagner, G. and Reinherz, E.L. (1998) Identification of a proline-binding motif regulating CD2-triggered T lymphocyte activation. *Proc. Natl Acad. Sci. USA* **95**, 14897–14902.

Okano, Y., Senshu, H., Hashimoto, M. *et al.* (2014) In planta recognition of a double-stranded RNA synthesis protein complex by a potexviral RNA silencing suppressor. *Plant Cell*, **26**, 2168–2183.

Ouibrahim, L., Mazier, M., Estevan, J., Pagny, G., Decroocq, V., Desbiez, C., Moretti, A., Gallois, J.L. and Caranta, C. (2014) Cloning of the Arabidopsis rwm1 gene for resistance to *Watermelon mosaic virus* points to a new function for natural virus resistance genes. *Plant J.* **79**, 705–716.

Ozeki, J., Takahashi, S., Komatsu, K., Kagiwada, S., Yamashita, K., Mori, T., Hirata, H., Yamaji, Y., Ugaki, M. and Namba, S. (2006) A single amino acid in the RNA-dependent RNA polymerase of Plantago asiatica mosaic virus contributes to systemic necrosis. *Arch. Virol.* **151**, 2067–2075.

Piron, F., Nicolaï, M., Minoïa, S., Piednoir, E., Moretti, A., Salgues, A., Zamir, D., Caranta, C. and Bendahmane, A. (2010) An induced mutation in tomato eIF4E leads to immunity to two potyviruses. *PLoS ONE*, **5**, e11313.

Pontier, D., Picart, C., Roudier, F. *et al.* (2012) NERD, a plant-specific GW protein, defines an additional RNAi-dependent chromatin-based pathway in Arabidopsis. *Mol. Cell* **48**, 121–132.

Postnikova, O.A. and Nemchinov, L.G. (2012) Comparative analysis of microarray data in Arabidopsis transcriptome during compatible interactions with plant viruses. *Virol. J.* **9**, 101.

Rate, D.N., Cuenca, J.V., Bowman, G.R., Guttman, D.S. and Greenberg, J.T. (1999) The gain-of-function Arabidopsis acd6 mutant reveals novel regulation and function of the salicylic acid signaling pathway in controlling cell death, defenses, and cell death. *Plant Cell*, **11**, 1695–1708.

Robaglia, C. and Caranta, C. (2006) Translation initiation factors: a weak link in plant RNA virus infection. *Trends Plant Sci.* **11**, 40–45.

Ruffel, S., Dussault, M.H., Palloix, A., Moury, B., Bendahmane, A., Robaglia, C. and Caranta, C. (2002) A natural recessive resistance gene against potato virus Y in pepper corresponds to the eukaryotic initiation factor 4E (eIF4E). *Plant J.* **32**, 1067–1075.

Ruffel, S., Gallois, J.L., Lesage, M.L. and Caranta, C. (2005) The recessive potyvirus resistance gene pot-1 is the tomato orthologue of the pepper pvr2-eIF4E gene. *Mol. Genet. Genomics* **274**, 346–353.

Sanfaçon, H. (2015) Plant translation factors and virus resistance. *Viruses*, **7**, 3392–3419.

Shimada, T.L., Shimada, T. and Hara-Nishimura, I. (2010) A rapid and non-destructive screenable marker, FAST, for identifying transformed seeds of Arabidopsis thaliana. *Plant J.* **61**(3), 519–528.

Takahashi, H., Kanayama, Y., Zheng, M.S., Kusano, T., Hase, S., Ikegami, M. and Shah, J. (2004) Antagonistic interactions between the SA and JA signaling pathways in Arabidopsis modulate expression of defense genes and gene-for-gene resistance to cucumber mosaic virus. *Plant Cell Physiol.* **45**, 803–809.

Truniger, N. and Aranda, M.A. (2009) Recessive resistance to plant viruses. *Adv. Virus Res.* **75**, 119–159.

Tsujimoto, Y., Numaga, T., Ohshima, K., Yano, M.A., Ohsawa, R., Goto, D.B., Naito, S. and Ishikawa, M. (2003) Arabidopsis TOBAMOVIRUS MULTIPLICATION (TOM) 2 locus encodes a transmembrane protein that interacts with TOM1. *EMBO J.* **22**, 335–343.

Uchida, N., Sakamoto, T., Kurata, T. and Tasaka, M. (2011) Identification of EMS-induced causal mutations in a non-reference Arabidopsis thaliana accession by whole genome sequencing. *Plant Cell Physiol.* **52**, 716–722.

Uknes, S., Mauch-Mani, B., Moyer, M., Potter, S., Williams, S., Dincher, S., Chandler, D., Slusarenko, A., Ward, E. and Ryals, J. (1992) Acquired resistance in Arabidopsis. *Plant Cell*, **4**, 645–656.

Wang, A. and Krishnaswamy, S. (2012) Eukaryotic translation initiation factor 4E-mediated recessive resistance to plant viruses and its utility in crop improvement. *Mol. Plant Pathol.* **13**, 795–803.

Yamaji, Y., Maejima, K., Ozeki, J. *et al.* (2012) Lectin-mediated resistance impairs plant virus infection at the cellular level. *Plant Cell*, **24**, 778–793.

Yamanaka, T., Ohta, T., Takahashi, M., Meshi, T., Schmidt, R., Dean, C., Naito, S. and Ishikawa, M. (2000) TOM1, an Arabidopsis gene required for efficient multiplication of a tobamovirus, encodes a putative transmembrane protein. *Proc. Natl Acad. Sci. USA* **97**, 10107–10112.

Yamanaka, T., Imai, T., Satoh, R., Kawashima, A., Takahashi, M., Tomita, K., Kubota, K., Meshi, T., Naito, S. and Ishikawa, M. (2002) Complete inhibition of tobamovirus multiplication by simultaneous mutations in two homologous host genes. *J. Virol.* **76**, 2491–2497.

Yang, P., Lüpken, T., Habekuss, A. *et al.* (2014) *PROTEIN DISULFIDE ISOMERASE LIKE 5-1* is a susceptibility factor to plant viruses. *Proc. Natl Acad. Sci. USA* **111**, 2104–2109.

Yoshii, M., Nishikiori, M., Tomita, K., Yoshioka, N., Kozuka, R., Naito, S. and Ishikawa, M. (2004) The Arabidopsis cucumovirus multiplication 1 and 2 loci encode translation initiation factors 4E and 4G. *J. Virol.* **78**, 6102–6111.